

Crumpled states of a wire in a cubic cavity with periodic obstaclesM. A. F. Gomes,¹ C. C. S. Pereira,² and V. P. Brito²¹*Departamento de Física, Universidade Federal de Pernambuco, 50670-901 Recife, Pernambuco, Brazil*²*Departamento de Física, Universidade Federal do Piauí, 64049-550 Teresina, Piauí, Brazil*

(Received 3 April 2012; revised manuscript received 14 November 2012; published 6 May 2013)

In this paper, we study experimentally the configurations of a plastic wire injected into a cubic cavity containing periodic obstacles placed along a fixed direction. The wire moves in a wormlike manner within the cavity until it becomes jammed in a crumpled state. The maximum packing fraction of the wire depends on the topology of the cavity, which in turn depends on the number of obstacles. The experimental results exhibit scaling laws and display similarities as well as differences with a recently reported two-dimensional version of this complex packing problem. We discuss in detail several aspects of this problem that seem as intricate as the problem of a self-avoiding random walk. Analogies between the experiment reported and some statistical aspects of the bond-percolation problem, as well as of the interacting electron gas at finite temperature, and other physical issues are also discussed.

DOI: [10.1103/PhysRevE.87.052103](https://doi.org/10.1103/PhysRevE.87.052103)

PACS number(s): 05.70.Np, 46.70.Hg, 62.20.F-, 68.65.-k

I. INTRODUCTION

In the past three decades the study of crumpled systems has deepened with emphasis on theoretical aspects of structures with a two-dimensional topology [1–18]. Moreover, a number of physical systems and physical processes involving crumpled structures of potential interest in technological applications have been discovered over the past years. As examples we can cite the experimental observation of crumpled conformations in aqueous suspensions of graphite oxide membranes [19], the study of acoustic emission in processes of crumpling using Mylar and paper sheets [20,21], the anomalous relaxation of strain and stress in crumpled sheets of Mylar and aluminum [22,23], the study of highly heterogeneous organic materials such as crumpled cream layers [24], and the synthesis of crumpled graphene sheets [25].

In contrast, the issue of crumpled structures with an effective one-dimensional topology such as nylon wires or threads where the length L is much larger than both transverse lengths has been less frequently studied. Crumpled wires appear to belong to a class of problems different from the self-avoiding walks, but with comparable difficulties and challenges. Anomalous physical properties in spherical structures of crumpled wires obtained by hand crumpling of a plastic wire were reported in the early 1990s [26–28]. The extension of those experimental studies to a crumpled wire confined in a two-dimensional cavity was shown to yield patterns of complex structure characterized by anomalous physical properties and robust scaling laws [29–34]. Furthermore, for this last two-dimensional version of crumpled wires, several authors have examined analogies with both a statistical field theory [35] and two-dimensional gravity [36]. Connections were made between experiments, simulations, and theory for crumpled wires and aspects of the packing of DNA in viral capsids [37–40]. Recently, electrical properties of graphite structures with nanometric height homologous to those of crumpled wires in two dimensions were reported [41].

The present work was inspired by a previous study [42] dealing with the problem of crumpled states of a wire in a two-dimensional cavity containing a periodic array of pins

whose height is equal to the diameter of the wire. The jamming limit of this nonthermal process was investigated as a function of the number of pins for different types of distributions of pins and cavity symmetries [42]. An analysis based on statistical thermodynamics was applied and it was shown that an absolute effective temperature T dependent on the packing density p can be introduced at the jamming limit, with T being a function that varies inversely with the number of pins n . Following this analysis, the entropy, the internal energy, and the free energy of the confined wire can be defined. As a result, a mean-field calculation suggests a connection of this problem with a Fermi gas with two-body interactions at low temperature as given by the Hartree-Fock theory in the sense that the total energy of the plastic wire confined in the cavity is proportional to the square of the effective temperature.

Here we extend the study of the packing of a plastic wire to a three-dimensional cubic cavity containing a regular array of metallic rods oriented in a single direction perpendicular to a pair of opposite faces. Moreover, the positions of the rods are defined by a square lattice. Naturally, other distributions of the metallic rods not studied in this paper are possible, for instance, cross rods in two and three directions. Beyond the intrinsic interest, the packing of a wire in a confined volume presents multiple analogies including (i) connections with the statistical properties of a trapped polymer chain in a porous medium [43–45], (ii) the packing of DNA in biological systems as viral capsids [46–48], (iii) the packing of DNA constrained to wrap around histone cores [49], (iv) the electrohydrodynamics of DNA in confined environments [50], and (v) the simulation of several process of packing in different effective temperatures. Additionally, crumpled wires confined in cells could find applications as chemical filters, heat exchangers, and catalytic converters. We would like to emphasize now the two fundamental differences between the problem that is examined in the present article and the two-dimensional problem studied previously in [42]. First, in the three-dimensional problem studied here there are entanglement effects of the wire that are absent in the two-dimensional problem. The use of cavities with rods in a single direction allows more freedom for the plastic wire to form entanglements as compared with other situations involving rods

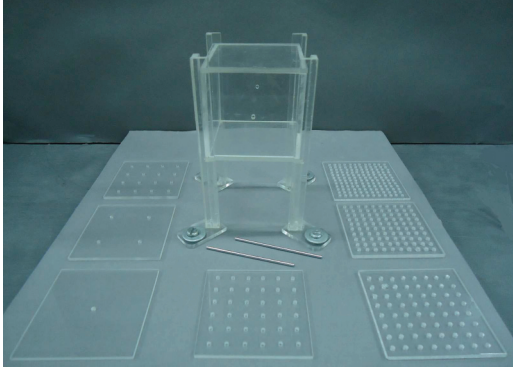


FIG. 1. (Color online) Cubic cavity of transparent acrylic with an internal volume of 6.0^3 cm^3 used in the packing experiment described in this paper. Two rods of steel wire with a diameter of 2.0 mm and seven perforated plates 3.0 mm thick for installation of n rods on the sites of a square lattice are shown. A total of 12 values of n were used, namely, 1, 4, 9, 16, 25, 36, 49, 64, 81, 100, 121, and 144.

distributed in more than one direction; hence this geometry is preferred here. Second, for the three-dimensional problem considered in the present study, the interaction of the wire with the obstacles cannot be neglected, as will be explained in Sec. IV.

This paper is organized as follows. The experimental details are described in Sec. II. A discussion of the results is presented in Sec. III. In Sec. IV the mean-field model introduced in [42] is applied in order to understand some of our findings in terms of statistical thermodynamics ideas. A brief summary of the paper and its main conclusions are given in Sec. V.

II. EXPERIMENTAL DETAILS

In our experiment the confining cell of cubic shape has an internal volume $L_0^3 = 60^3 \text{ mm}^3$. The faces of the cavity are made of transparent acrylic 3 mm thick and the rods are cylindrical pieces of a steel wire 2 mm in diameter with an effective length L_0 within the cavity [i.e., a total length of $(L_0 + 6)$ mm including the fitting in the faces of the cavity]. These rods are fixed in the positions defined by a square lattice, all pointing in the same direction perpendicular to a pair of opposite faces. The forced injection of the wire is made perpendicular to the rods using two small holes localized at the center of two parallel opposite faces. Figure 1 illustrates the cubic cell and some rods and perforated plates to fix the steel rods. The experiment uses cavities with twelve distributions of rods ($n = 1, 4, 9, 16, 25, 36, 49, 64, 81, 100, 121, \text{ and } 144$ rods). In addition, a control group of eight crumpled wires in cavities free of rods was also investigated. The position of the rods is defined by dividing the area of each of two opposite faces of the cavity L_0^2 in n equal nonoverlapping and contiguous squares of area L_0^2/n . Each rod is placed in the geometric center of those squares and so the nearest-neighbor rod-rod distance between the center of the rods is $\ell = L_0/n^{1/2}$. In order to reduce the friction, all parts of the cavity are polished. The cavity and wire operated in a dry regime, free of any lubricant. The plastic wire used in the packing was an indoor telephone cable commonly used in telephonic wiring, with diameter

$\zeta = 1 \text{ mm}$. This type of cable is divided in a core of tinned copper 0.4 mm in diameter and PVC coverage 0.3 mm thick.

Each experiment begins by fitting a straight wire in the opposite apertures and subsequently pushing manually and uniformly the wire on both sides of the cell toward the interior of the cavity in the horizontal direction defining the injection axis. Uniformity in the packing operation is guaranteed by the low injection velocity at each channel, which was of the order of 1 cm/s, as estimated by the average time spent reaching the jammed packing density in each case. Typically this time was of the order of 10 (30) min for cavities with the higher (lower) number of rods. As observed for two-dimensional cavities, for wires with the largest lengths, the crumpled structures formed become rigid. However, differently from the packing of wire in a two-dimensional cavity, in the present case the difficulty in the injection increases steadily and the injection velocity goes to zero with the formation of a jammed state of crumpled wire within the cavity. The packing process proceeds from the outer rods close to the faces of the cavity to the central part of the cell. The observed phenomena are widely independent of the injection speed for all intervals of injection velocity compatible with a manual process. Figures 2(a)–2(f) illustrate the morphologies of configurations of the plastic wire obtained at the maximum packing fraction for an even number of rods: $n = 4$ [Fig. 2(a)], $n = 16$ [Fig. 2(b)], $n = 36$ [Fig. 2(c)], $n = 64$ [Fig. 2(d)], $n = 100$ [Fig. 2(e)], and $n = 144$ [Fig. 2(f)]. In all these images the injection axis lies along the horizontal. The length L of the wire in the interior of the cavity in the jammed state is associated with the corresponding three-dimensional packing fraction p ($0 \leq p \leq 1$) through the relation $p = \pi \zeta^2 L / 4L_0^3$. Thus the packing fraction at the beginning of each experiment is $p = p_{\min} = \pi \zeta^2 / 4L_0^2$. Ensembles with eight equivalent configurations of three-dimensional crumpled wires were used in this work for each cavity with a fixed number of rods.

For an odd number n of rods there is a fundamental difference from the situation in which n is an even number: In the first case there is a row of $n^{1/2}$ rods just in front of the injection axis. Because of this, we show separately in Fig. 3 typical configurations of the crumpled states of a wire in a three-dimensional cavity for $n = 9$ [Fig. 3(a)], $n = 25$ [Fig. 3(b)], $n = 49$ [Fig. 3(c)], $n = 81$ [Fig. 3(d)], and $n = 121$ [Fig. 3(e)].

As can be observed from Figs. 2 and 3, in contrast to the two-dimensional case, the wire within the three-dimensional cavity is, in general, in an entangled state. Only in Fig. 2(f), corresponding to the maximum number of rods $n = 144$, do we observe a less entangled structure. The basic geometric units of the crumpled wires examined in the present paper are loops of wires, although these loops lack planarity and present a somewhat more diversified repertoire of forms when compared with the two-dimensional case. In the next section we will estimate the average size of such loops in this problem using simple mean-field arguments derived from a detailed exam of the morphology of the structures of the three-dimensional crumpled wires. As stated above, the packing of a wire in a three-dimensional cavity presents frequently the phenomenon of irreversible formation of entanglements: With the increase in the packing fraction of wire within the cavity, the number of loops increases and the probability of one or more loops to cross another loop

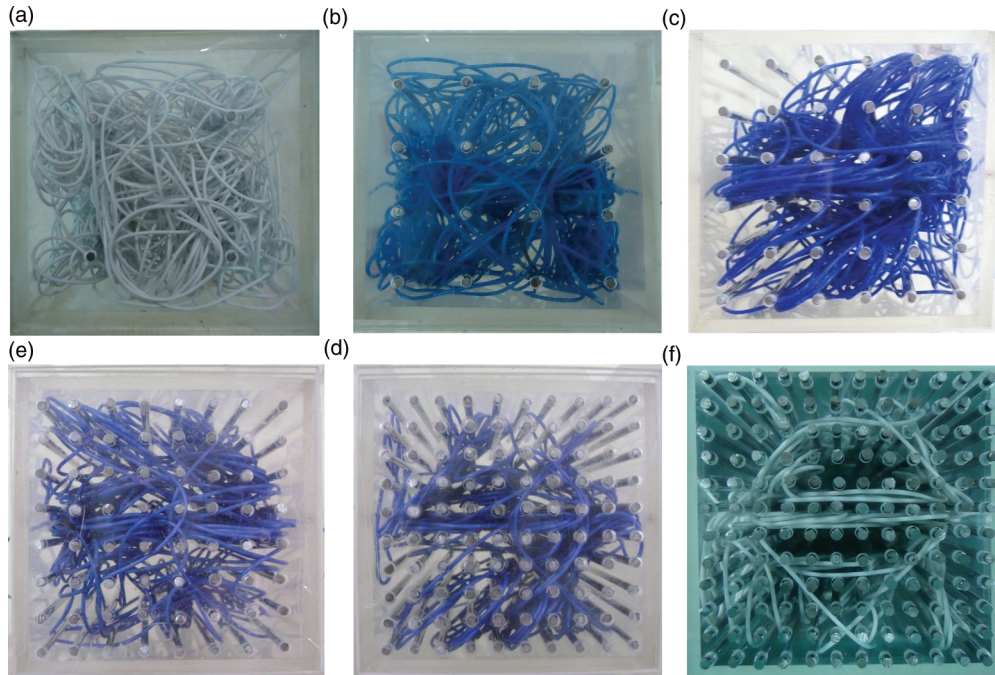


FIG. 2. (Color online) Typical three-dimensional configurations of crumpled wires obtained with the cubic cavity shown in Fig. 1 for an even number of rods: (a) $n = 4$, (b) $n = 16$, (c) $n = 36$, (d) $n = 64$, (e) $n = 100$, and (f) $n = 144$. The injection axis is located in the horizontal.

increases; this phenomenon gives origin to the entanglements observed in the structures of three-dimensional crumpled wires. As a consequence, frequently it is impossible to extract the wire from the cavity through simple pulling operations. The occurrence of this entanglement phenomenon is important in many fields, including surgical operations with a catheter [51].

III. RESULTS AND DISCUSSION

In principle, the packing fraction of the wire within the cavity must decrease on average with an increase in the number of rods n due to geometric hindrance factors. However, oscillations in the packing fraction $p(n)$ are observed with $p(n)$ odd occupying local maxima, whereas the packing fractions

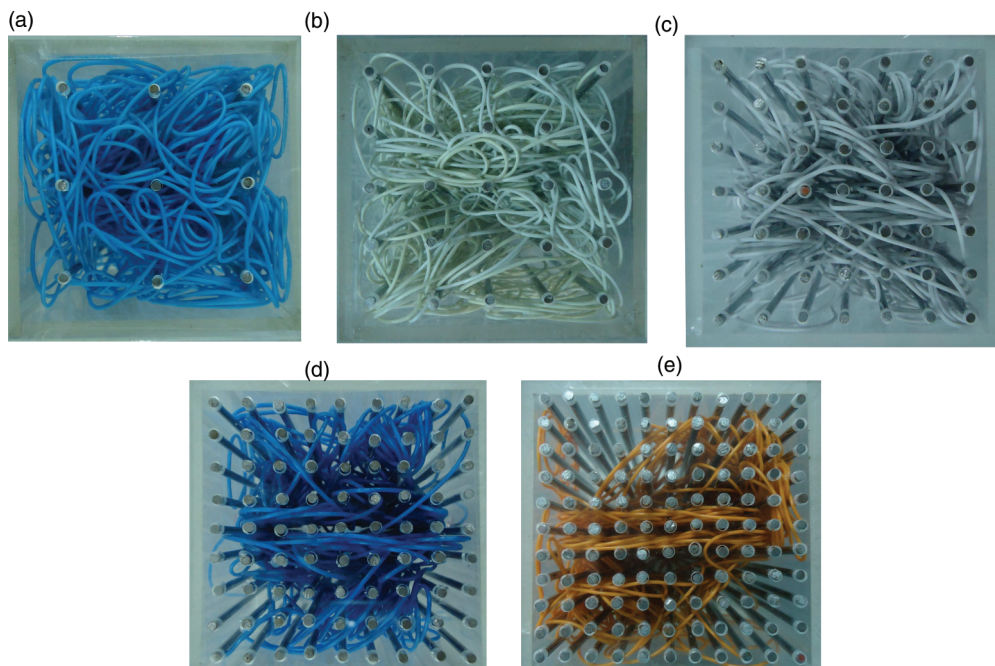


FIG. 3. (Color online) Same as in Fig. 2, but for an odd number of rods: (a) $n = 9$, (b) $n = 25$, (c) $n = 49$, (d) $n = 81$, and (e) $n = 121$. The injection axis is located in the horizontal.

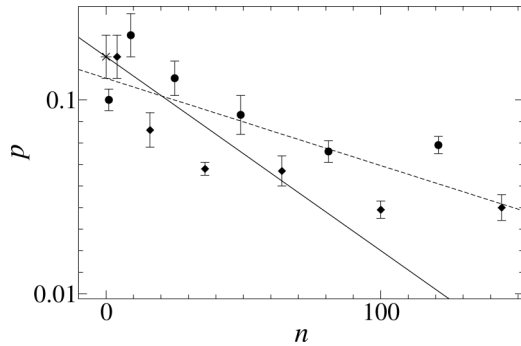


FIG. 4. Average packing density $p(n)$ for crumpled wires jammed in a cubic cavity with rods for n odd (\bullet), n even (\blacklozenge), and $n = 0$ ($*$). The continuous (dashed) line represents the argument of the constant capacity of the cavity (best fit to the data). See Sec. III.

for even values of n occupy local minima. These oscillations can be expected because for n odd there is a row of $n^{1/2}$ rods along the injection channels, as noticed in the previous section. This fact introduces a fundamental geometric difference: If n is even, the axis of injection is completely free of obstacles. These oscillations in the packing density are shown in Fig. 4, which presents alternating minima and maxima of $p(n)$ for n even and odd, respectively, provided $n \geq 4$. Oscillations in the packing density were observed in other dense packings, e.g., in packings of congruent disks in a circle [52]. The region with $n \leq 4$ is peculiar: Surprisingly, the packing density obtained with the cavity with four rods, $p(4)$, is equal to the density for a cavity free of rods, $p(0)$, and both are 20% larger than the corresponding density for the cavity with a single rod, $p(1) = 0.100 \pm 0.005$. That is, to attain higher packing densities, one rod just along the injection line is less effective than four rods distributed in the symmetric configuration of Fig. 2(a) but leaving the injection line free of obstacles. Apparently, the single central rod is more effective in scattering the wire from the central region of the cavity, creating there an exclusion zone.

A detailed examination of Figs. 2 and 3 shows that for small values of the number of rods the crumpled structures form an entangled and diffuse state not too compact, but tending to obliterate the vision of the opposite face of the cavity. This is particularly true in Figs. 2(a) ($n = 4$) and 3(a) ($n = 9$). The blockage effect is more efficient when the number of rods n is odd, as a consequence of the tendency of $p(n)$ to exhibit maxima when n is odd. As shown in Fig. 4, the packing density presents local maxima for an odd number of rods, that is, $p(i^2) > p((i-1)^2)$ and $p((i+1)^2)$ for i an odd integer with $n = i^2 \geq 9$. For the group of cavities with the number of rods $n = 16, 36, 64, 100$, and 144 [Figs. 2(b)–2(f)] there is a transparency in the structures of wire formed that allow us to discern some parts of the opposite face of the cavity, a tendency that evidently increases with the number of rods. Another aspect observed is a clear concentration of braided structures of wire along the injection axis. With the subgroup of cavities with $36, 64, 100$, and 144 rods [Figs. 2(c)–2(f)] a third characteristic emerges in the packing of wires, which is the tendency to form lateral arms made of wire whose angle with the injection axis is approximately 45° . This effect is particularly pronounced for $n = 100$ [Fig. 2(e)] and $n = 144$

[Fig. 2(f)]. The existence of arms of wire forming 45° with the injection axis is almost absent for n odd, with the exception of the situation illustrated in Fig. 3(e). A detailed examination of Figs. 2 and 3 suggests that, in general, the distributions of rods with n odd ($\neq 1$) (that is, $n = 9, 25, 49, 81$, and 121) are more efficient to scatter the wire in different directions, leading to an increase in the number of accessible states of the wire, as compared with the distributions with an even number of rods.

On average, the maximum (minimum) packing fraction due to the crumpled wire found in the experiment is 0.13 ± 0.01 (0.049 ± 0.004) for $n = 9$ ($n = 100$), corresponding on average to a length L of plastic wire introduced in the cavity of $35\ 800$ mm ($13\ 500$ mm). The volumetric fraction occupied by rods, $p_{\text{rods}} = n\pi\xi^2/L_0^2$, in the experiment varies in the interval $0 \leq p_{\text{rods}} \leq 0.125$ and then the cavities work in the regime of high porosity $1 - p_{\text{rods}} \geq 0.875$. As a consequence, a variation of 12.5% in the porosity due to the rods implies a highly nonlinear variation of $\Delta = 265\%$ in the packing density of the wire [$\Delta = (0.13/0.049) \times 100 = 265\%$]. It is worth mentioning that the total occupancy P of the cavity by both the wire and rods has a maximum value P_{max} for the configurations with $n = 121$: $P_{\text{max}} = [p(\text{crumpled wire}) = 0.079 \pm 0.005] + (p_{\text{rods}} = 0.106) = 0.185 \pm 0.005$ [Fig. 3(e)]. This is interesting and counterintuitive at first sight because such a configuration suggests a less pronounced occupancy of the cavity when compared, for instance, with Fig. 3(a). The reason for this apparent discrepancy is that Fig. 3(a), for $n = 9$ rods, has a low fraction of the space occupied by the rods and the fuzzy structure of the crumpled wire is efficient to spread in the cavity along all directions, creating the impression that it occupies almost entirely the interior of the cavity. Only as a matter of comparison do we note that the packing densities of the crumpled wire in the range 0.05 – 0.10 obtained in 9 of a total of 13 situations studied here correspond to the packing densities of new snow and settling snow, respectively [53].

It is known that percolation provides a very simple model of random media with enough realism to make relevant predictions [54]. Furthermore, percolation is a source of intuition for studying more complicated critical phenomena. In this sense a numerical comparison between percolation and packing of wires is interesting in this paragraph and in the next one. Due to the fact that percolation clusters and crumpled wires divide some important geometrical characteristics, as the topological dimension, the fractal dimension, and the diffusion exponent, it was conjectured that both structures can belong to the same universality class [31]. Within this context, it is interesting to notice that the total occupation fraction found above ($P_{\text{max}} = 0.185 \pm 0.005$), for $n = 121$, is close within statistical uncertainties to the percolation threshold for the bond-percolation problem in a three-dimensional bcc lattice [$p_c(\text{bond, bcc}) = 0.180\ 287\ 5 \pm 0.000\ 001\ 0$ [55]]. For $n = 144$ rods, with a total occupation fraction of $P = 0.180 \pm 0.006$, the agreement is almost perfect. The remaining 11 configurations with $n = 0$ – 100 have an average total packing fraction of 0.12 ± 0.02 , a concentration that is equal within statistical fluctuations to the bond-percolation threshold for the three-dimensional fcc lattice [$p_c(\text{bond, fcc}) = 0.120\ 163\ 5 \pm 0.000\ 001\ 0$ [55]]. Of course, the periodic distributions of rods used in this

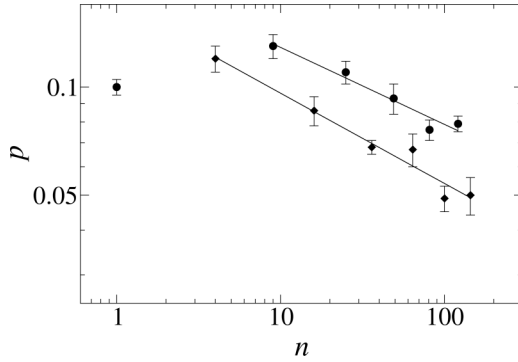


FIG. 5. Same density $p(n)$ as in Fig. 4, but for log-log scales. In this case the packing density is described by the best fit $p \sim n^{-0.25}$ ($p \sim n^{-0.21}$) for n even (odd).

work do not define three-dimensional lattices with bcc or fcc symmetry and the numerical comparisons discussed above must be seen as giving merely effective values. Approximately 100 additional packing experiments with cavities of aspect ratio $60 < L_0/\zeta < 180$ were unable to surpass the maximum average packing density $P_{\max} = 0.185 \pm 0.005$ previously reported, a result that suggests that the saturation value for the packing fraction should have been reached.

Each averaged experimental packing fraction of the wire, $p(n)$, is associated with a typical fluctuation bar with magnitude $\delta(n)$ and the relative fluctuation averaged over all n is $\langle \delta(n)/p(n) \rangle = 0.078$, or 7.8%. A simple way to try to derive the dependence of p with n shown in Fig. 4 would be to assume that the three-dimensional cavity has a fixed packing capacity as given by the sum rule, [(packing density of the plastic wire) $\equiv p(n)$] + [(packing density due to the n rods) $\equiv p_{\text{rods}}(n)$] = $C = \text{const}$, or in terms of the variables involved, $p(n) + \pi n \zeta^2 / L_0^2 = C$, where in the last expression we have used the fact that the rods have diameter 2ζ . Thus, in this approximation, $p(n)$ would decay linearly with n as $p(n) = C - \pi n \zeta^2 / L_0^2 \approx C - 0.0009n$. In this case we should expect that $C = p(n=0) = 0.12 \pm 0.01$ as obtained directly from the experiment and consequently $p(n) = 0.12 - 0.0009n$. The straight line obtained with this argument of fixed maximum capacity is shown in Fig. 4 (continuous line); it gives a crude approximation to the experimental data, within typical relative fluctuations of 12%, between $n = 0$ and 64. These relative fluctuations are approximately 54% higher than the value $\langle \delta(n)/p(n) \rangle$ found for the typical fluctuations in the measurement of the packing densities. In contrast, the linear best fit to the experimental data as obtained for all values of n from 0 to 144 gives $p(n) = C_0 - 0.0004n$, with $C_0 = 0.110$, and a coefficient of correlation of 0.802 (dashed line in Fig. 4); i.e., it presents a decay rate close to the half of that predicted by the argument of the constant capacity. This coefficient C_0 , which corresponds to the packing fraction for the wire in a cavity free of rods, is equal to the bond-percolation probability for the fcc lattice within an uncertainty of 8%.

A nonlinear dependence of the packing fraction of the crumpled wire with the number of rods in the three-dimensional case studied in the present paper seems more reasonable than the linear dependence discussed in the previous paragraph. In Fig. 5 we show a double logarithmic plot of the packing density

of the plastic wire with the associated power-law fits: This quantity exhibits the scaling $p = kn^{-\alpha}$, with $k = 0.17$ (0.21) and $\alpha = 0.25$ (0.21) for n even (odd) within typical relative uncertainties of these parameters of 5%–10%. The coefficients of correlation are 0.982 (0.993) for the number of rods n even (odd), respectively. Thus p scales approximately as $p \sim n^{-1/4}$, although with different values of k depending on whether the number of rods n is even or odd; i.e., the distribution of packing densities $p(n)$ in three dimensions has a heavy tail when compared with the two-dimensional case. A rough estimate of the exponent α can be made following the same heuristic mean-field reasoning applied in the two-dimensional case [42]. Here the argument reads as follows: The expected maximum packing density of the crumpled wire in the three-dimensional cavity with rods obeys the dependence $p \sim N\lambda\zeta^2/L_0^3$, where N is the corresponding number of loops of wire within the cavity and λ is the typical size of these loops. A detailed examination of all experimental configurations shown in Figs. 2 and 3 [more clearly in Figs. 2(c)–2(e) and 3(c)–3(e)] suggests that each loop spans a prismatic sector of the cavity whose typical smallest length is of the order of the separation between contiguous rods (ℓ) and the remaining two transversal lengths define an area of the order of $L_0 \times L_0$. Taking λ as the geometric mean of these three lengths ℓ, L_0 , and L_0 and using $N \sim (\text{volume}) \sim L_0^3$, we get finally $p \sim \lambda\zeta^2 \sim (\ell L_0^2)^{1/3} \zeta^2 \sim (L_0^3/n^{1/2})^{1/3} \zeta^2 \sim n^{-1/6}$ or $p \sim n^{-0.17}$. This last result is reasonably close to the experimental scaling $p \sim n^{-0.21}$ observed in Fig. 5 for n odd within uncertainties of 10% in both exponents.

The corresponding packing density $p(n)$ obtained in the two-dimensional case for cavities and distributions of pins of diversified symmetries [42] is given by $p(n) \sim n^{-\alpha}$, for packing almost free of finite-size effects, with α close to $\frac{3}{4}$ within uncertainties of 10%. It can be noticed that in three dimensions even for the configuration with the largest packing fraction [Fig. 3(a)] the wire touches only marginally the boundaries of the cavity, preferring to be accommodated mainly in the interior of cavity and close to the injection axis. This last aspect is particularly clear in Figs. 2(c)–2(f) and 3(c)–3(e). In other words, the distribution of rods is quite efficient to screen the outer faces of the cavity from contact with the crumpled wire. This is reasonable because we know that crumpled wires in three dimensions tend to distribute itself in space obeying the mass M size R scaling $M \sim R^D$, with D close to 2.75 within uncertainties of 5% for different types of crumpling procedures that not involve cavities with obstacles [26,38,40]. This means that as the size R increases, the average density of the wire that is localized in the outer regions tends to zero as $\rho \sim M/R^3 \sim R^{D-3} \sim R^{-0.25}$. For comparison, the self-avoiding random walk (SARW), with the same topology of the crumpled wire and excluded-volume effects as well, obeys $M \sim R^{5/3}$ and consequently $\rho \sim R^{-4/3}$. Thus crumpled wires and the SARW are in completely different universality classes.

A last intriguing aspect that we would like to comment on in this section concerns a particular characteristic of the packing density $p(n)$ shown in Fig. 5: In contrast to what happens in the two-dimensional case [42], $p(n)$ does not present any abrupt change as the number of pins n varies when a discontinuity occurs in the first derivative of this function. We conjecture that in the two-dimensional case the observed change in the behavior of $p(n)$ for $n \approx 16$ (Figs. 3 and 4 in [42]) is somewhat

analogous to a type of Kosterlitz-Thouless (KT) transition in which there are two regimes of different elastic behavior [56]. When applied to the two-dimensional crumpled states of a wire in a cavity with pins, we observe that for a small number of pins $n < 16$ we have a less rigid or softer structure with loops of several sizes distributed in a highly heterogeneous or disordered configuration through the cavity [Figs. 1(a)–1(c) in Ref. [42]]; this corresponds to the high-temperature disordered phase [42]. However, for a large number of pins $n > 16$ the structure of loops is clearly much more rigid and the disorder decreases. In this last case the configurations are characterized by a stack of loops along the injection channel with a not too large variation in size [Figs. 1(e)–1(i) in [42]]; this corresponds to the low-temperature quasicrystalline phase [42]. We know that a true KT transition does not occur in three dimensions and it is just this absence of transition that is observed in the problem of the crumpled states of a wire in a cavity with rods studied in the present paper. This is reflected in the behavior of $p(n)$, which decreases in a well behaved way as shown in Fig. 5.

IV. MEAN-FIELD MODEL

In this section we present a straightforward discussion of several aspects of our experiment using ideas from statistical thermodynamics and mean-field arguments. Before we go into the details of the mean-field model we can ask why this model is introduced here and why it is expected to work. Our justification is that crumpled wires have formal analogies with nonbranched polymers such as the one-dimensional topology, the existence of entropic aspects, and also the occurrence of self-avoiding interactions. We know that mean-field models belong to the simplest class of models successfully used in polymeric systems [43]. Furthermore, the use of a mean-field model for the problem of the two-dimensional packing of a wire in a cavity with pins [42] has led to some interesting insight into this problem. In contrast, we know that mean-field theories work better in higher dimensions than in lower and thus we should expect that the application of such arguments in our three-dimensional system can also be successful. Formal analogies between nonthermal crumpling and thermodynamics are explored in this article within the same theoretical framework introduced in [42] for the two-dimensional case. In that case, for a sufficiently large concentration of pins there is a jamming (equilibrium) state characterized by the simple morphology of a linear wire perfectly stretched along the two injection channels, with a packing concentration p_{\min} . As a consequence, the number of states accessible to the wire is $\Omega(p_{\min}) = 1$ and the entropy of those states satisfies $S(p_{\min}) \sim \ln \Omega(p_{\min}) = 0$, with $p_{\min} = \zeta/L_0 \rightarrow 0$ in the thermodynamic limit, i.e., for a cavity of infinite size $L_0 \rightarrow \infty$. This situation corresponds to an effective temperature $T = 0$. In three dimensions the exact limit $T = 0$ is impossible because if the separation between the centers of the nearest-neighbor rods is 3ζ , the extreme condition that allows the introduction of the wire within the cavity, a complex morphology of the crumpled wire of the type discussed in [29,30] can again be obtained. This structure is restricted to a quasi-two-dimensional slice of the cavity limited by two adjacent parallel planes of rods separated by a free distance ζ and close to the symmetry plane of the cavity

containing the injection axis. As a consequence we expect that the minimum temperature in the three-dimensional case could never reach zero. A second expectation is the existence of two branches for the entropy function $S(p)$ or, equivalently, of two branches for the number of accessible states $\Omega(p)$ depending on whether the number of rods is even or odd. We should expect that $\Omega(p; n \text{ odd}) > \Omega(p; n \text{ even})$ due to the existence of the row of rods along the injection channels for n odd as described in Secs. II and III. If n is odd, Ω tends to be larger for two reasons. First, in this case the number of initial states of the wire in the beginning of the packing process increases because now a left-right symmetry associated with the initial positioning of the wire in the cavity appears. Of course, in this case many more complex initial states are possible, e.g., meandering states of the wire along the different units of the central row of rods. Second, as noted in the beginning of Sec. III, the distributions of rods with n odd are more efficient in increasing the number of possibilities for the wire to be distributed within the cavity.

In contrast, if the number of rods decreases in general, i.e., for n even or odd, the constraints on the motion of the wire within the cavity decrease as well and more equivalent configurations are accessible to the wire. In this case we expect that the entropy increases as a consequence. This reasoning suggests that we can associate with our nonthermal system an effective temperature that decreases when the number of rods increases. In the nonthermal packing of a wire studied here the fluctuations are induced by the driving force of injection in several equivalent experiments and do not arise obviously from random thermal motion. For simply connected cavities free of rods we get the high- (infinite-) temperature limit of the system. However, for a finite density of rods, for both branches of $p(n)$ shown in Fig. 5, in the interval $4 < n < 144$, we reach progressively the low-temperature limit of the system if n increases. For a very high number of rods, the temperature T approaches a minimum value different from zero, as will be quantified below. Many recent works have proposed that nonequilibrium systems experiencing jamming or structural arrest could be described by equilibrium thermodynamic concepts and an effective disorder temperature could be introduced to characterize the properties of such systems [57,58].

Using simple heuristic mean-field arguments as done in [42], we now introduce an effective internal energy per unit of volume E for a wire confined in a cavity with n fixed rods and an effective Helmholtz free energy $F = E - TS$. Evidently, for E two contributions are important:

$$E = E_{\text{wire-wire}} + E_{\text{wire-rods}}, \quad (1)$$

where the first term $E_{\text{wire-wire}}$ is a repulsive energy due to excluded-volume interactions between different parts of the crumpled wire, as long as we can neglect the elastic energy of curvature for a plastic wire. The second term $E_{\text{wire-rods}}$ can be neglected in the two-dimensional case: It is a repulsive energy due to excluded-volume interactions between different parts of the crumpled wire and the rods. As the packing fraction of wire, $p = \pi \zeta^2 L / 4L_0^3$, is a measure of the mean local concentration of mass of the wire, the average repulsive energy per unit volume $E_{\text{wire-wire}}$ is assumed to be a two-body interaction proportional to the number of pairs of interacting pieces of the

wire, i.e., to p^2 : $E_{\text{wire-wire}} = \varepsilon p^2$. In contrast, for interactions between the wire and rods, we adopt $E_{\text{wire-rods}} = \xi p p_{\text{rods}}$, where $p_{\text{rods}} = \pi \zeta^2 n L_0 / L_0^3 = \pi \zeta^2 n / L_0^2$ is the density of rods (whose diameter, as previously explained in Sec. II, is $2\zeta = 2$ mm). The constants ε and ξ are expected to have similar numerical values. From these definitions we can see easily that the energy term $E_{\text{wire-rods}}$ could be neglected in Eq. (1) if $4nL_0/L \ll 1$. This limit is not satisfied in our experiment, where this ratio averaged over all n is $\langle 4nL_0/L \rangle \approx 3.4$.

Furthermore, as observed in [42], the entropy S per unit volume of the wire within the cavity must, of course, be an extensive function, i.e., it depends linearly on the total length of the wire $S \sim L \sim p$. That is, the entropy S is proportional to the (jammed) packing fraction of the plastic wire within the cavity and decays smoothly with the number of rods within the cavity: $S = \sigma p$, where σ is a constant. Moreover, there are two branches for the entropy S depending on whether the number of rods n is even or odd, with $S(n \text{ even}) < S(n \text{ odd})$, as expected from the discussion in the beginning of this section. Consequently, the free energy of the crumpled wire in a three-dimensional cavity with rods reads

$$F = E - TS = \varepsilon p^2 + \zeta p p_{\text{rods}} - T \sigma p, \quad (2)$$

where the effective temperature T will be found. In the minimization of F , when p varies, the first and second terms, due to self-exclusion, favor small values of p or L , while the second term, due to entropy $-TS$, favors naturally large values of p or L . Thus $\partial F / \partial p = 0$ leads to the equilibrium (jamming) condition

$$p = (T\sigma - \zeta p_{\text{rods}}) / 2\varepsilon. \quad (3)$$

After substitution of (3) in (1) we get for the internal energy at equilibrium a quadratic function of the temperature, in agreement with the two-dimensional case [42]:

$$E = (\sigma^2 T^2 - \zeta^2 p_{\text{rods}}^2) / 4\varepsilon. \quad (4)$$

From the last results the expressions for the entropy and the specific heat at equilibrium can be obtained as usual through $S = -(\partial F / \partial T)_V$ and $C_V = (\partial E / \partial T)_V$, i.e., they are both linear functions in T as found in [42] for the two-dimensional case. The definition of the effective temperature emerges from (3) after substitution of the experimental result $p = kn^{-1/4}$ discussed in the previous section:

$$T = (2\varepsilon p + \zeta p_{\text{rods}}) / \sigma = A\delta^{-1/4} + B\delta, \quad (5)$$

with $A = (2\varepsilon k / L_0^{1/2} \sigma)$, $B = \xi \pi \zeta^2 / \sigma$, and $\delta = n / L_0^2$ the number of rods per unit area. Thus, in the limit $\zeta \rightarrow 0$ the effective temperature T always increases as the number of rods per unit area decreases, $T \sim A\delta^{-1/4}$, with $T \rightarrow \infty$ when the density of rods goes to zero, as expected on the basis of Ref. [42]. In contrast, if the interaction between the wire and rods can be neglected (i.e., if $\xi \rightarrow 0$) and ζ and L_0 are finite, T and n (or δ) are equally related through the same power-law dependence, i.e., $T \sim \delta^{-1/4}$. The effective temperature measures the disorder of the wire in the cavity: As long as the density of rods increases, the average heterogeneity in the packing decreases and more regular structures appear as in the typical configurations shown in Figs. 2 and 3, especially in Figs. 2(f) and 3(e).

In summary, the results obtained here for the internal energy, entropy, and specific heat for the crumpled wire in the jamming state are analogous to those found in [42], i.e., they are analogous to the results known for a Fermi gas with two-body interactions at low temperature as derived from the Hartree-Fock theory [59]. Thus, as obtained with this type of gas, if the dimensionality varies, the temperature dependence of the basic thermodynamic quantities associated with our system remains the same.

V. CONCLUSION

We studied experimentally a complex packing problem in three dimensions. It involves crumpled structures formed when a plastic wire is injected into cubic cavities with different topologies formed by different distributions of n rods localized on square lattices. This article extends a previous work on the packing of a crumpled wire in a two-dimensional cavity with fixed pins [42]. It was found that the packing density p of the wire obeys different scaling functions (depending on n being even or odd): $p \sim n^{-\alpha}$, with α typically in the interval 0.20–0.25; a heuristic estimation of the value of this exponent was also discussed. Simple mean-field arguments suggest a relation between the topology of the cavity as given by the number of rods with an effective absolute temperature for this nonthermal system. Additionally, we have confirmed that the analogy with the Fermi gas with two-body forces at finite temperature, developed in [42] for a two-dimensional version of the packing problem, maintains its validity in three dimensions. Another interesting subject is the existence of similarities between crumpled wires and the bond-percolation problem [31]; several aspects of these two problems were discussed.

We conjecture that the phenomenon reported in the present paper is essentially independent of the details of the geometry of the distribution of rods within the cavity as well as of the symmetry of the cavity as already observed in the two-dimensional problem discussed in [42]; i.e. the results would be dependent only on the topology or the number of rods within the cavity. Our focus was on the basic physical (geometrical) properties of crumpled structures. However, beyond this intrinsic interest, the packing of a wire in a confined space presents multiple interests including connections with the statistical properties of a polymer or a self-avoiding walk in a medium with obstacles [43–45] and the packing of DNA in many biological situations [46–50]. From a technological point of view, crumpled wires confined in cavities could find applications as, e.g., chemical filters, heat exchangers, catalytic converters, and targeted drug delivery units.

We believe that an additional effort in terms of theory and numerical simulations must be made to investigate the experimental scaling behaviors reported here as well as to refine the possible connections of the problem discussed in this article at a heuristic level with other fundamental problems in physics including percolation and self-avoiding walks. Furthermore, investigation of other versions of the problem studied here with different distributions of rods defining different symmetries is also a very important matter in order to test universality in this class of systems.

ACKNOWLEDGMENTS

We acknowledge CAPES, CNPq, FAPEPI, PRONEX, UFPE, and UFPI for financial support. M.A.F.G. thanks

Professor M. Engelsberg and G. L. Vasconcelos for comments on the manuscript.

-
- [1] M. A. F. Gomes, *Am. J. Phys.* **55**, 649 (1987).
 [2] Y. Kantor, M. Kardar, and D. R. Nelson, *Phys. Rev. Lett.* **57**, 791 (1986).
 [3] M. A. F. Gomes, T. I. Jyh, T. I. Ren, I. M. Rodrigues, and C. B. S. Furtado, *J. Phys. D* **22**, 1217 (1989).
 [4] M. A. F. Gomes, T. I. Jyh, and T. I. Ren, *J. Phys. A: Math. Gen.* **23**, L1281 (1990).
 [5] A. Lobkovsky, S. Gentges, H. Li, D. Morse, and T. A. Witten, *Science* **270**, 1482 (1995).
 [6] F. Plouraboué and S. Roux, *Physica A* **227**, 173 (1996).
 [7] M. Ben Amar and Y. Pomeau, *Proc. R. Soc. London Ser. A* **453**, 729 (1997).
 [8] E. Cerda, S. Chaieb, F. Melo, and L. Mahadevan, *Nature (London)* **401**, 46 (1999).
 [9] S. C. Venkataramani, *Nonlinearity* **17**, 301 (2004).
 [10] D. L. Blair and A. Kudrolli, *Phys. Rev. Lett.* **94**, 166107 (2005).
 [11] E. Sultan and A. Boudaoud, *Phys. Rev. Lett.* **96**, 136103 (2006).
 [12] G. A. Vliegthart and G. Gomper, *Nat. Mater.* **5**, 216 (2006).
 [13] T. A. Witten, *Rev. Mod. Phys.* **79**, 643 (2007).
 [14] I. Dierking and P. Archer, *Phys. Rev. E* **77**, 051608 (2008).
 [15] T. Tallinen, J. A. Åström, and J. Timonen, *Nat. Mater.* **8**, 25 (2009).
 [16] H. Aharoni and E. Sharon, *Nat. Mater.* **9**, 993 (2010).
 [17] A. S. Balankin, D. S. Ochoa, I. A. Miguel, J. P. Ortiz, and M. Á. Martínez Cruz, *Phys. Rev. E* **81**, 061126 (2010).
 [18] W. Bai, Y.-C. Lin, T.-K. Hou, and T.-M. Hong, *Phys. Rev. E* **82**, 066112 (2010).
 [19] X. Wen, C. W. Garland, T. Hwa, M. Kardar, E. Kokufuta, Y. Li, M. Orkisz, and T. Tanaka, *Nature (London)* **355**, 426 (1992).
 [20] E. M. Kramer and A. E. Lobkovsky, *Phys. Rev. E* **53**, 1465 (1996).
 [21] P. A. Houle and J. P. Sethna, *Phys. Rev. E* **54**, 278 (1996).
 [22] K. Matan, R. B. Williams, T. A. Witten, and S. R. Nagel, *Phys. Rev. Lett.* **88**, 076101 (2002).
 [23] R. F. Albuquerque and M. A. F. Gomes, *Physica A* **310**, 377 (2002).
 [24] M. A. F. Gomes, C. C. Donato, S. L. Campelo, R. E. de Souza, and R. Cassia-Moura, *J. Phys. D* **40**, 3665 (2007).
 [25] G. Wang, J. Yang, J. Park, X. Gou, B. Wang, H. Liu, and J. Yao, *J. Phys. Chem. C* **112**, 8192 (2008).
 [26] J. Albino Aguiar, M. A. F. Gomes, and A. S. Neto, *J. Phys. A: Math. Gen.* **24**, L109 (1991).
 [27] M. A. F. Gomes, F. F. Lima, and V. M. Oliveira, *Philos. Mag. Lett.* **64**, 361 (1991).
 [28] J. B. C. Garcia, M. A. F. Gomes, T. I. Jyh, and T. I. Ren, *J. Phys. A: Math. Gen.* **25**, L353 (1992).
 [29] C. C. Donato, M. A. F. Gomes, and R. E. de Souza, *Phys. Rev. E* **66**, 015102(R) (2002).
 [30] C. C. Donato, M. A. F. Gomes, and R. E. de Souza, *Phys. Rev. E* **67**, 026110 (2003).
 [31] C. C. Donato, F. A. Oliveira, and M. A. F. Gomes, *Physica A* **368**, 1 (2006).
 [32] C. C. Donato and M. A. F. Gomes, *Phys. Rev. E* **75**, 066113 (2007).
 [33] N. Stoop, F. K. Wittel, and H. J. Herrmann, *Phys. Rev. Lett.* **101**, 094101 (2008).
 [34] Y. C. Lin, Y. W. Lin, and T. M. Hong, *Phys. Rev. E* **78**, 067101 (2008).
 [35] L. Boué and E. Katzav, *Europhys. Lett.* **80**, 54002 (2007).
 [36] B. Carneiro da Cunha, *Europhys. Lett.* **88**, 31001 (2009).
 [37] E. Katzav, M. Adda-Bedia, and A. Boudaoud, *Proc. Natl. Acad. Sci. USA* **103**, 18900 (2006).
 [38] M. A. F. Gomes, V. P. Brito, and M. S. Araújo, *J. Braz. Chem. Soc.* **19**, 293 (2008).
 [39] M. A. F. Gomes, V. P. Brito, A. S. O. Coelho, and C. C. Donato, *J. Phys. D* **41**, 235408 (2008).
 [40] N. Stoop, J. Najafi, F. K. Wittel, M. Habibi, and H. J. Herrmann, *Phys. Rev. Lett.* **106**, 214102 (2011).
 [41] M. A. F. Gomes, R. R. Hora, and V. P. Brito, *J. Phys. D* **44**, 255401 (2011).
 [42] M. A. F. Gomes, V. P. Brito, M. S. Araújo, and C. C. Donato, *Phys. Rev. E* **81**, 031127 (2010).
 [43] P.-G. de Gennes, *Scaling Concepts in Polymer Physics* (Cornell University Press, Ithaca, 1979).
 [44] M. Rubinstein, *Phys. Rev. Lett.* **57**, 3023 (1986); **59**, 1946 (1987).
 [45] G. W. Slater and S. Y. Wu, *Phys. Rev. Lett.* **75**, 164 (1995).
 [46] P. K. Purohit, M. M. Inamdar, P. D. Grayson, T. M. Squires, J. Kondev, and R. Phillips, *Biophys. J.* **88**, 851 (2005).
 [47] A. S. Petrov, M. B. Boz, and S. C. Harvey, *J. Struct. Biol.* **160**, 241 (2007).
 [48] Y. Hu, R. Zandi, A. Anavitarte, C. M. Knobler, and W. M. Gelbart, *Biophys. J.* **94**, 1428 (2008).
 [49] C. Vaillant, B. Audit, and A. Arnéodo, *Phys. Rev. Lett.* **95**, 068101 (2005).
 [50] O. B. Bakajin, T. A. J. Duke, C. F. Chou, S. S. Chan, R. H. Austin, and E. C. Cox, *Phys. Rev. Lett.* **80**, 2737 (1998).
 [51] J. F. Brichant, V. Bonhomme, and P. Hans, *Int. J. Obstet. Anesth.* **15**, 159 (2006).
 [52] R. L. Graham, B. D. Lubachevsky, K. J. Nurmela, and P. R. J. Östergård, *Discrete Math.* **181**, 139 (1998).
 [53] R. Barry and T. Y. Gan, *The Global Cryosphere, Past, Present and Future* (Cambridge University Press, Cambridge, 2011).
 [54] D. Stauffer, *Introduction to Percolation Theory* (Taylor & Francis, London, 1985).
 [55] C. D. Lorenz and R. M. Ziff, *Phys. Rev. E* **57**, 230 (1998).
 [56] J. M. Kosterlitz and D. J. Thouless, *J. Phys. C* **6**, 1181 (1973).
 [57] N. Xu and C. S. O'Hern, *Phys. Rev. Lett.* **94**, 055701 (2005).
 [58] E. Bouchbinder, *Phys. Rev. E* **77**, 051505 (2008).
 [59] A. L. Fetter and J. D. Walecka, *Quantum Theory of Many-Particle Systems* (McGraw-Hill, New York, 2003).